



Aqueous phase (catalytic) wet air oxidation of ammonia: Thermodynamic considerations

Cédric Lousteau, Hana Ayadi, Claude Desorme *

Institut de recherches sur la catalyse et l'environnement de Lyon (IRCELYON), UMR5256 CNRS – Université Claude Bernard Lyon 1, 2 avenue Albert Einstein, 69626 Villeurbanne Cedex, France

ARTICLE INFO

Article history:

Received 5 July 2016

Received in revised form 26 August 2016

Accepted 3 September 2016

Available online 5 September 2016

Keywords:

Ammonia

Catalytic wet air oxidation

Thermodynamics

Equilibria

Reactivity

ABSTRACT

The equilibrium concentrations in ammonia and ammonium ion in the liquid and gas phases could be calculated in the temperature range 25–250 °C, under typical operating conditions for the catalytic wet air oxidation of ammonia. A satisfactory agreement was obtained with the data collected upon blank experiments as well as in the presence of unreactive catalyst supports. Thermodynamic calculations appeared to be crucial to access a better comprehension of the reaction mixture composition under catalytic wet air oxidation reaction conditions, especially the ammonia partition and speciation among the different phases. New insights were gained in terms of ammonia reactivity.

© 2016 Elsevier B.V. All rights reserved.

1. Introduction

Ammonia is being produced in large amounts for many different applications (e.g. fertilizers, nitric acid, cooling fluid, plastics, synthetic fibers and resins, explosives). The estimated world production of ammonia reached 146 million tons in 2015 [1]. It is mainly produced from molecular nitrogen and hydrogen via the Haber Bosch process. As a result, ammonia might be transferred to the atmospheric and aquatic environments, which represents a major risk both in terms of public health and environment (eutrophication, acidic rains). Ammonia release might also derive from the decomposition, oxidation or reduction of higher nitrogen-containing molecules. While a number of approaches has been developed to treat gaseous ammonia, via adsorption and/or oxidation, only a limited number of research works has been devoted to the treatment of ammonia in the liquid phase directly. Moreover, the most developed process in this later case is the stripping: the ammonia molecule is then transferred to the gas phase before being treated [2]. In addition, adsorption (clinoptilolite) [3,4], biological treatments (nitration-denitrification [5], Anammox [6]) and advanced oxidation processes (ozonation [7,8], photocatalysis [9,10]) showed some major limitations either in terms of efficiency, cost and/or selectivity toward molecular nitrogen vs. nitrites and/or nitrates.

To overcome such limitations, some attention has more recently been paid to the catalytic wet air oxidation process. Important improvements have been obtained with the implementation of supported noble metal catalysts [11–15], especially in terms of efficiency and selectivity.

However, the catalytic wet air oxidation reaction being carried out in a three-phase reactor, a better understanding and description of the gas-liquid and liquid–liquid thermodynamic equilibria is necessary. Indeed, such knowledge is required in order to be able to accurately describe the ammonia catalytic wet air oxidation reaction mechanism and further extract the true kinetics for the different processes involved. Insights could also be gained on how to improve the reactivity of ammonia upon catalytic wet air oxidation.

As the result, the objective of this preliminary study was to determine the partition of ammonia between the gas and liquid phases and, in the liquid phase, the speciation between ammonia and ammonium ion, as a function of temperature in the range 25–250 °C. The results of our calculations were then valuably compared with experimental data acquired in the catalytic wet air oxidation of ammonia upon blank experiments and/or in the presence of inert catalyst supports.

2. Materials and methods

Thermodynamic calculations were performed in order to monitor (i) the evolution of the equilibrium concentrations in ammonia

* Corresponding author.

E-mail address: claude.desorme@ircelyon.univ-lyon1.fr (C. Desorme).

Table 1

Analytical conditions for the ion chromatography measurements.

Column	Cations	Anions
Metrosep C4 150/4.0		Metrosep A Supp 5 150/4.0
Stationary phase	Silica gel grafted with carboxylic functional groups	Polyvinyl alcohol with quaternary ammonium groups
Elutant composition	HNO_3 (1.7 mmol L ⁻¹) + dipicholinic acid (0.7 mmol L ⁻¹)	Na_2CO_3 (3.2 mmol L ⁻¹) + NaHCO_3 (1 mmol L ⁻¹)
Elutant flow rate (mL min ⁻¹)	0.9	0.7
Working pressure (MPa)	6	9

($[\text{NH}_3]_l$, $[\text{NH}_3]_g$) and ammonium ion ($[\text{NH}_4^+]_l$) in the liquid and gas phases, respectively; and (ii) the changes in pH as a function of temperature. The initial conditions of the system were set as in the experimental tests ($[\text{NH}_3]_0 = 60 \text{ mmol L}^{-1}$; $T = 25^\circ\text{C}$; $V_l = 150 \text{ mL}$; $V_g = 123 \text{ mL}$). To perform the calculations, the nitrogen mass balance (Eq. (1)) and the electro neutrality equation (Eq. (2)) were considered, as well as the variation with temperature of the acid-base constant (K_b , Eq. (3)), the self-ionization constant of water (K_w , Eq. (4)) and the Henry's constant (K_H or K_H^{cc} , Eqs. (5) and (6), respectively).

$$[\text{NH}_3]_0 V_l = [\text{NH}_3]_g V_g + [\text{NH}_3]_l V_l + [\text{NH}_4^+]_l V_l \quad (1)$$

$$[\text{NH}_4^+]_l + [\text{H}_3\text{O}^+]_l = [\text{OH}^-]_l \quad (2)$$

$$K_b = \frac{[\text{NH}_4^+]_l [\text{OH}^-]_l}{[\text{NH}_3]_l} \quad (3)$$

$$K_w = [\text{H}_3\text{O}^+]_l [\text{OH}^-]_l \quad (4)$$

$$K_H = \frac{[\text{NH}_3]_l}{P_{\text{NH}_3}} \quad (5)$$

$$K_H^{cc} = \frac{[\text{NH}_3]_l}{[\text{NH}_3]_g} = K_H \times RT \quad (6)$$

with $R = 0.0821 \text{ L atm mol}^{-1} \text{ K}^{-1}$ and T in Kelvin.

Moreover, for the calculations, the binary solution of ammonia in water was considered to be infinitely diluted. Indeed, the concentration in water was 55.5 mol L⁻¹, while the concentration in ammonia was 60 mmol L⁻¹. As a result, the Raoult law and the simplified Duperray's empirical law (Eq. (7)) could be accurately applied to calculate the water vapor pressure ($P_{\text{H}_2\text{O}}$) in equilibrium with the liquid at a given temperature (T).

$$P_{\text{H}_2\text{O}} = \left(\frac{T}{100} \right)^4 \quad (7)$$

with T in Celsius in the range 100–250 °C.

Similarly, the solute (ammonia) was assumed to follow Henry's law (Eqs. (5) or (6)).

Finally, for comparison/validation purposes, preliminary tests were performed in a 273 mL batch reactor made of Hastelloy C22 equipped with a magnetically driven stirrer. In a typical run, 150 mL of a 60 mmol L⁻¹ ammonia solution (Sigma Aldrich, 28–30 vol.% NH₃) was initially loaded into the autoclave. After purging the reactor with argon several times, to eliminate any trace of oxygen, a 4 bar residual pressure of argon was maintained in the reactor to avoid any boiling phenomenon upon heating the solution up to the desired reaction temperature. The reactor was subsequently heated up to 200 °C under continuous stirring (1200 rpm). The time when air was introduced in the autoclave, to reach 50 bar total pressure (34 bar of synthetic air, i.e. 6.8 bar of oxygen), was considered as zero time for the reaction. All along the reaction, liquid samples were periodically withdrawn from the reactor and analyzed to measure the total nitrogen content in the solution (TN), the pH of the solution at atmospheric pressure and ambient temperature and the ammonia, nitrites and nitrates concentrations in the liquid phase.

Table 2
Ammonia acid-base constant (K_b).

T(°C)	T(K)	pK _b ^a	K _b ^a	pK _b ^b	K _b ^b
25	298	4.751	1.774×10^{-5}	4.753	1.765×10^{-5}
30	303	4.740	1.820×10^{-5}	4.742	1.810×10^{-5}
35	308	4.733	1.849×10^{-5}	4.734	1.843×10^{-5}
40	313	4.730	1.862×10^{-5}	4.729	1.865×10^{-5}
45	318	4.726	1.879×10^{-5}	4.727	1.874×10^{-5}
50	323	4.723	1.892×10^{-5}	4.727	1.873×10^{-5}
75	348			4.763	1.726×10^{-5}
100	373			4.845	1.429×10^{-5}
125	398			4.963	1.089×10^{-5}
150	423			5.110	7.771×10^{-6}
175	448			5.280	5.253×10^{-6}
200	473			5.470	3.385×10^{-6}
225	498			5.681	2.085×10^{-6}
250	523			5.912	1.223×10^{-6}

^a R.G. Bates, G.D. Pinching, Journal of American Chemical Society, 72 (3) (1950) 1393–1396.

^b J.R. Fisher, H.L. Barnes, The Journal of Physical Chemistry, 76 (1) (1972) 90–99 [Data were recalculated using Helgeson's full equation and the five parameters fitted by the authors].

The liquid samples were analyzed by ion chromatography (Metrohm 881 IC Pro) with an automated sampler (863Compact Autosampler, 36 positions) and two distinct conductivity detectors for the anions and the cations, respectively. The characteristics for the two different separation columns and the corresponding mobile phases used for the analysis of both the anions (NO_2^- , NO_3^-) and the cations (NH_4^+) are presented in Table 1. Calibration curves in the range below 10 mg L⁻¹ were established using NH_4Cl (Normapur 99.5%), NaNO_3 (Sigma-Aldrich > 99%) and NaNO_2 (Sigma-Aldrich > 97%). In addition, the total nitrogen content (TN) in the liquid samples was measured using a TOC-VCSH analyzer coupled with a TN unit (TNM-1) from Shimadzu. In our study, TN corresponds to the total nitrogen content in ammonium, nitrites and nitrates. The nitrogen balance could be assessed from the comparison between the TN values and the ion chromatography results.

3. Results and discussion

3.1. Thermodynamic calculations

To start with, a throughout survey of the literature was performed in order to collect all the data already available concerning the ammonia acid-base constant (K_b) [16,17], the self ionization constant of water (K_w) [17–20] and the Henry's constant for ammonia (K_H , K_H^{cc}) [21,22]. Several sources could be identified in the literature for such data. These data are summarized in Tables 2–4, respectively. While the values collected for K_b and K_w were quite numerous and totally coherent, much scarce data could be directly found for K_H and/or K_H^{cc} .

In addition to the very limited data provided by Jones et al. at 149, 175, 203 and 245 °C [21], the raw data provided by Sander et al. (K_H^0 and $\frac{-d \ln K_H}{d(\frac{1}{T})}$) had to be reprocessed [22]. Since the values for K_H^0 varied between 10 and 78 mol L⁻¹ atm⁻¹ and the values for $\frac{-d \ln K_H}{d(\frac{1}{T})} = \frac{\Delta_{\text{sol}} H}{R}$ varied between 1500 and 4400 K,

Table 3Water self-ionization constant (K_w).

T(°C)	T(K)	K_w^a	pK_w^a	K_w^b	pK_w^b	K_w^c	pK_w^c	K_w^d	pK_w^d
25	298	1.008×10^{-14}	14.00			1.00×10^{-14}	14.00	9.93×10^{-15}	14.00
30	303	1.460×10^{-14}	13.84					1.44×10^{-14}	13.84
35	308	2.081×10^{-14}	13.68					2.05×10^{-14}	13.69
40	313	2.916×10^{-14}	13.54					2.86×10^{-14}	13.54
45	318	4.019×10^{-14}	13.40					3.94×10^{-14}	13.40
50	323	5.469×10^{-14}	13.26			5.50×10^{-14}	13.26	5.34×10^{-14}	13.27
55	328	7.297×10^{-14}	13.14					7.13×10^{-14}	13.15
60	333	9.637×10^{-14}	13.02					9.38×10^{-14}	13.03
75	348					2.00×10^{-13}	12.70	1.99×10^{-13}	12.70
100	373			6.76×10^{-13}	12.17	5.50×10^{-13}	12.26	5.57×10^{-13}	12.25
125	398			1.05×10^{-12}	11.98	1.23×10^{-12}	11.91	1.25×10^{-12}	11.90
150	423			1.91×10^{-12}	11.72	2.29×10^{-12}	11.64	2.33×10^{-12}	11.63
175	448			3.72×10^{-12}	11.43	3.80×10^{-12}	11.42	3.78×10^{-12}	11.42
200	473			5.37×10^{-12}	11.27	5.50×10^{-12}	11.26	5.46×10^{-12}	11.26
225	498					7.24×10^{-12}	11.14	7.14×10^{-12}	11.15
250	523					8.91×10^{-12}	11.05		

^a H.S. Harned, W.J. Hamer, Journal of American Chemical Society, 55(6) (1933) 2194–2206.^b J.V. Dobson, H.R. Thirsk, Electrochimica Acta, 16 (1971) 315–338.^c J.R. Fisher, H.L. Barnes, The Journal of Physical Chemistry, 76 (1) (1972) 90–99.^d C. Tsonopoulos, D.M. Coulson, L.B. Inman, Journal of Chemical and Engineering Data, 21 (2) (1976) 190–193.**Table 4**Henry's constants for ammonia (K_H^0 , $\frac{-d \ln K_H}{d(\frac{1}{T})}$, K_H , K_H^{cc}).

T(°C)	T(K)	K_H^{cc} ^a	K_H ^b (mol L ⁻¹ atm ⁻¹)	K_H^{cc} ^b
25	298	57.31	1402.08	
50	323	21.03	557.64	
60	333	14.69	401.55	
75	348	8.91	254.62	
77	350	8.36	240.35	
100	373	4.24	129.76	
125	398	2.21	72.28	
149	422	45.45	1.27	44.15
150	423		1.25	43.30
175	448	27.03	0.75	27.56
200	473		0.48	18.46
203	476	17.86	0.45	17.64
225	498		0.32	12.90
245	518	11.11	0.23	9.95
250	523		0.22	9.35

^a M.E. Jones, The Journal of Physical Chemistry, 67 (5) (1963) 1113–1115.^b R. Sander, Compilation of Henry's Law Constants for Inorganic and Organic Species of Potential Importance in Environmental Chemistry, Air Chemistry Department, Max-Planck Institute of Chemistry (1999) <http://www.henrys-law.org/henry-3.0.pdf>.

depending on the authors, the average values were calculated after eliminating the upper and lower extreme values. We obtained $K_H^0 = 57.31 \text{ mol L}^{-1} \text{ atm}^{-1}$ and $\frac{-d \ln K_H}{d(\frac{1}{T})} = \Delta_{sol}H = 3860.00 \text{ K}$. Then, Eq. (8) was used in order to recalculate $K_H(T)$ in the full range of temperature from 25 till 250 °C.

$$K_H(T) = K_H^0 \times \exp \left[\frac{\Delta_{sol}H}{R} \left(\frac{1}{T} - \frac{1}{T^0} \right) \right] = K_H^0 \times \exp \left[\frac{-d \ln K_H}{d(\frac{1}{T})} \left(\frac{1}{T} - \frac{1}{T^0} \right) \right] \quad (8)$$

with K_H^0 , the Henry's constant at 25 °C; $\Delta_{sol}H$, the enthalpy of solution, $R = 0.0821 \text{ L atm mol}^{-1} \text{ K}^{-1}$ and T in Kelvin ($T^0 = 298 \text{ K}$).

Subsequently, K_H^{cc} was recalculated from Eq. (6). Although a reasonable agreement was observed between the two sets of data, an important uncertainty was remained in the determination of the gas phase composition because of huge distribution of the values for K_H^0 and $\frac{-d \ln K_H}{d(\frac{1}{T})}$.

For a better visualization, the evolution of those three constants (K_b , K_w , K_H^{cc}) as a function of temperature, in the range 25–250 °C, is shown on Figs. 1–3, respectively. It is observed that the $\text{NH}_3/\text{NH}_4^+$

acid-base equilibrium is shifted toward left, i.e. toward ammonia (NH_3) as the temperature increased. On the opposite, the ionization of water (K_w) rapidly increased as a function of temperature, indicating that the ionization of water is favored at higher temperature. Finally, the Henry's constant, expressed as K_H^{cc} , was shown to decrease drastically as the temperature increased from 25 to 100 °C, showing that ammonia stripping toward the gas phase will be favored at higher temperature.

In the following, all the calculations were performed using the average values for $K_H^0 = 57.31 \text{ mol L}^{-1} \text{ atm}^{-1}$ and $\frac{-d \ln K_H}{d(\frac{1}{T})} = \Delta_{sol}H = 3860.00 \text{ K}$ derived from the results published by Sander et al. [22].

The equilibrium concentrations in $[\text{NH}_3]_l$, $[\text{NH}_3]_g$ and $[\text{NH}_4^+]$ were calculated in the temperature range 25–250 °C following an iterative process:

- the temperature was fixed (T) and the corresponding values for K_b , K_w and K_H^{cc} were extracted from Tables 2–4, respectively;
- the pH was arbitrarily fixed at 1;
- the concentration in hydronium ion in the liquid phase ($[\text{H}_3\text{O}^+]$) was calculated using Eq. (9);

$$[\text{H}_3\text{O}^+]' = 10^{-pH} \quad (9)$$

- the concentration in hydroxide ion in the liquid phase ($[\text{OH}^-]$) was calculated from Eq. (4);
- the concentration in ammonium ion in the liquid phase ($[\text{NH}_4^+]$) was derived from Eq. (2);
- the concentration in ammonia in the liquid phase ($[\text{NH}_3]$) was extracted from Eq. (3);
- the concentration in ammonia in the gas phase ($[\text{NH}_3]_g$) was deduced from Eq. (6);

For a given temperature (T), fixed at step i, the process was continued by incrementing the pH (step ii) and recalculating all concentrations (step iii–vii), until the calculated concentrations in nitrogen species satisfied Eq. (1), with $[\text{NH}_3]_0 = 60 \text{ mmol L}^{-1}$; $V_l = 150 \text{ mL}$ and $V_g = 123 \text{ mL}$.

Once the system was solved for a given temperature, the temperature was incremented and the iterations started again (step ii–vii) to explore the full temperature range 25–250 °C.

An example for the iterations performed at $T = 200 \text{ }^\circ\text{C}$, using $K_b = 3.385 \times 10^{-6}$, $K_w = 5.44 \times 10^{-12}$ (average value) and $K_H^{cc} = 18.46$

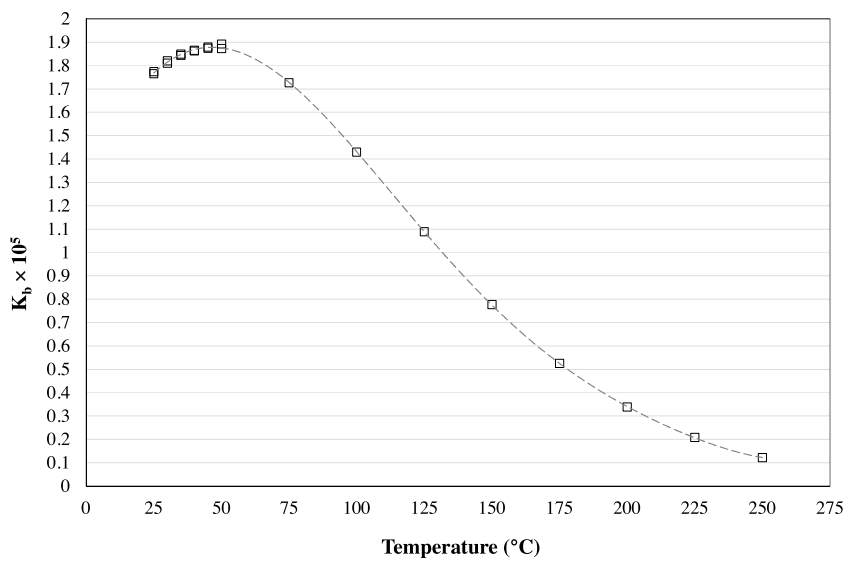


Fig. 1. Evolution of the ammonia acid-base constant (K_b) as a function of temperature, in the range 25–250 °C.

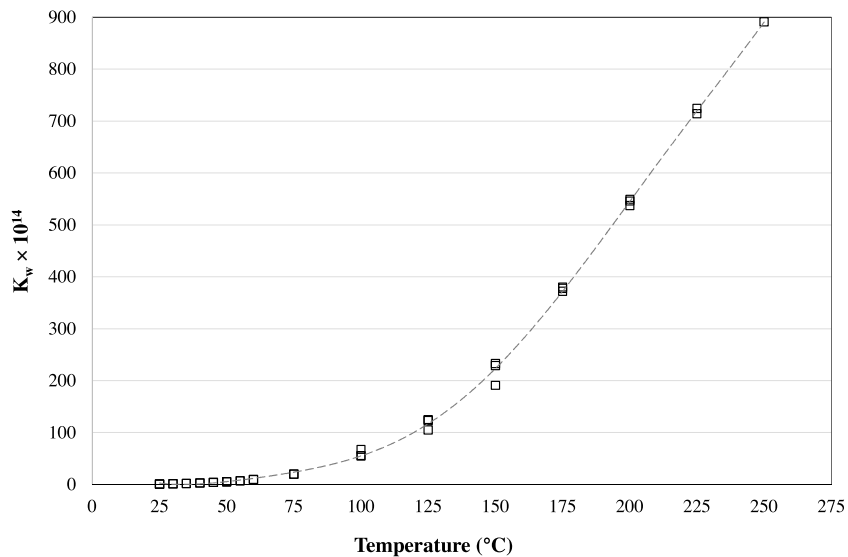


Fig. 2. Evolution of the self-ionization constant of water (K_w) as a function of temperature, in the range 25–250 °C.

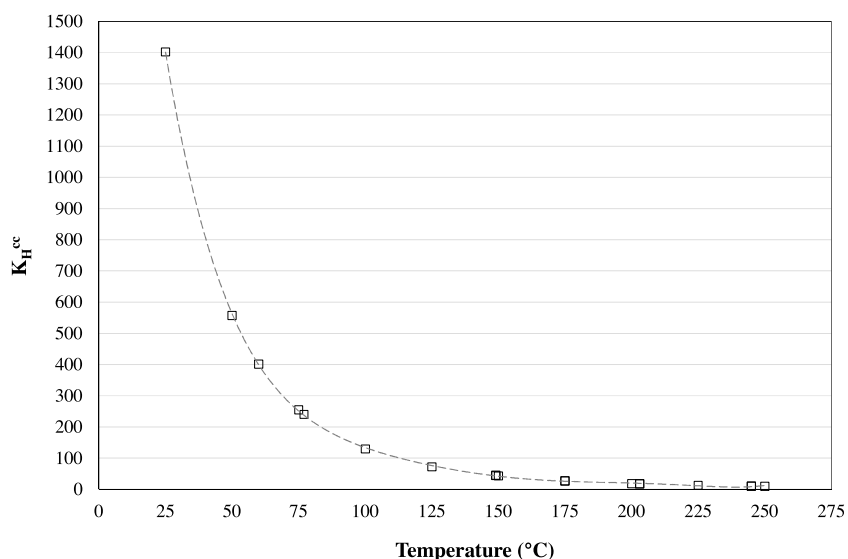


Fig. 3. Evolution of the Henry's constant for ammonia (K_H^{cc}) as a function of temperature, in the range 25–250 °C.

Table 5

Example of an iterative calculation of $[H_3O^+]$, $[OH^-]$, $[NH_4^+]$, $[NH_3]$, and $[NH_3]_g$ performed at 200 °C until the mass balance was fulfilled ($K_b = 3.385 \times 10^{-6}$, $K_w = 5.44 \times 10^{-12}$, $K_H^{cc} = 18.46$, $[NH_3]_0 = 60 \text{ mmol L}^{-1}$; $V_l = 150 \text{ mL}$, $V_g = 123 \text{ mL}$).

pH	Concentrations (mmol L ⁻¹)					
	$[H_3O^+]$	$[OH^-]$	$[NH_4^+]$	$[NH_3]$	$[NH_3]_g$	$[NH_3]_0$
1	1.000×10^2	5.440×10^{-8}	-1.000×10^2	-1.607×10^{-3}	-8.706×10^{-5}	-100.00
2	1.000×10^1	5.440×10^{-7}	-1.000×10^1	-1.607×10^{-3}	-8.706×10^{-5}	-10.00
3	1.000×10^0	5.440×10^{-6}	-1.000×10^0	-1.607×10^{-3}	-8.706×10^{-5}	-1.00
4	1.000×10^{-1}	5.440×10^{-5}	-9.995×10^{-2}	-1.606×10^{-3}	-8.701×10^{-5}	-0.10
5	1.000×10^{-2}	5.440×10^{-4}	-9.456×10^{-3}	-1.520×10^{-3}	-8.232×10^{-5}	-0.01
6	1.000×10^{-3}	5.440×10^{-3}	4.440×10^{-3}	7.135×10^{-3}	3.865×10^{-4}	0.01
7	1.000×10^{-4}	5.440×10^{-2}	5.430×10^{-2}	8.726×10^{-1}	4.727×10^{-2}	0.97
7.1	7.943×10^{-5}	6.849×10^{-2}	6.841×10^{-2}	1.384×10^0	7.497×10^{-2}	1.51
7.2	6.310×10^{-5}	8.622×10^{-2}	8.616×10^{-2}	2.194×10^0	1.189×10^{-1}	2.38
7.3	5.012×10^{-5}	1.085×10^{-1}	1.085×10^{-1}	3.479×10^0	1.885×10^{-1}	3.74
7.4	3.981×10^{-5}	1.366×10^{-1}	1.366×10^{-1}	5.515×10^0	2.987×10^{-1}	5.90
7.5	3.162×10^{-5}	1.720×10^{-1}	1.720×10^{-1}	8.741×10^0	4.735×10^{-1}	9.30
7.6	2.512×10^{-5}	2.166×10^{-1}	2.165×10^{-1}	1.385×10^1	7.505×10^{-1}	14.69
7.7	1.995×10^{-5}	2.726×10^{-1}	2.726×10^{-1}	2.196×10^1	1.190×10^0	23.21
7.8	1.585×10^{-5}	3.432×10^{-1}	3.432×10^{-1}	3.480×10^1	1.885×10^0	36.69
7.9	1.259×10^{-5}	4.321×10^{-1}	4.321×10^{-1}	5.516×10^1	2.988×10^0	58.04
7.901	1.256×10^{-5}	4.331×10^{-1}	4.331×10^{-1}	5.541×10^1	3.002×10^0	58.31
7.902	1.253×10^{-5}	4.341×10^{-1}	4.341×10^{-1}	5.567×10^1	3.016×10^0	58.58
7.903	1.250×10^{-5}	4.351×10^{-1}	4.351×10^{-1}	5.593×10^1	3.030×10^0	58.85
7.904	1.247×10^{-5}	4.361×10^{-1}	4.361×10^{-1}	5.619×10^1	3.044×10^0	59.12
7.905	1.245×10^{-5}	4.371×10^{-1}	4.371×10^{-1}	5.645×10^1	3.058×10^0	59.39
7.906	1.242×10^{-5}	4.381×10^{-1}	4.381×10^{-1}	5.671×10^1	3.072×10^0	59.66
7.907	1.239×10^{-5}	4.391×10^{-1}	4.391×10^{-1}	5.697×10^1	3.086×10^0	59.94
7.9071	1.239×10^{-5}	4.392×10^{-1}	4.392×10^{-1}	5.699×10^1	3.087×10^0	59.96
7.9072	1.238×10^{-5}	4.393×10^{-1}	4.393×10^{-1}	5.702×10^1	3.089×10^0	59.99
7.90721	1.238×10^{-5}	4.393×10^{-1}	4.393×10^{-1}	5.702×10^1	3.089×10^0	59.99
7.90722	1.238×10^{-5}	4.394×10^{-1}	4.393×10^{-1}	5.703×10^1	3.089×10^0	60.00
7.90723	1.238×10^{-5}	4.394×10^{-1}	4.394×10^{-1}	5.703×10^1	3.089×10^0	60.00
7.90724	1.238×10^{-5}	4.394×10^{-1}	4.394×10^{-1}	5.703×10^1	3.089×10^0	60.00
7.90725	1.238×10^{-5}	4.394×10^{-1}	4.394×10^{-1}	5.703×10^1	3.090×10^0	60.01
8	1.000×10^{-5}	5.440×10^{-1}	5.440×10^{-1}	8.742×10^1	4.736×10^0	91.85

is presented in **Table 5**. Of course, the negative values of the concentrations calculated at the lowest pH are not feasible and must be discarded. The most approached solution indicated that the equilibrium concentrations at 200 °C were $[H_3O^+]$ = 1.238×10^{-5} mmol L⁻¹, $[OH^-]$ = 4.394×10^{-1} mmol L⁻¹, $[NH_4^+]$ = 4.394×10^{-1} mmol L⁻¹, $[NH_3]$ = 5.703×10^1 mmol L⁻¹ and $[NH_3]_g$ = 3.089 mmol L⁻¹ and that the pH decreased down to ca. 7.91.

All equilibrium concentrations, i.e. $[H_3O^+]$, $[OH^-]$, $[NH_4^+]$, $[NH_3]$, and $[NH_3]_g$ and the corresponding pH values in the temperature range 25–250 °C are summarized in **Table 6**.

Finally, for a better understanding and given our experimental conditions ($[NH_3]_0 = 60 \text{ mmol L}^{-1}$; $V_l = 150 \text{ mL}$, $V_g = 123 \text{ mL}$), the number of mole of ammonium ion and ammonia in the different phases could be calculated according to Eqs. (10)–(12).

$$n(NH_4^+) = [NH_4^+] \times V_l \quad (10)$$

$$n(NH_3)_l = [NH_3]_l \times V_l \quad (11)$$

$$n(NH_3)_g = [NH_3]_g \times V_g \quad (12)$$

The evolutions of the number of mole $n(NH_4^+)$, $n(NH_3)_l$ and $n(NH_3)_g$ as a function of the reaction temperature are presented on **Figs. 4–6**, respectively. The corresponding values are also summarized in **Table 7**. The evolution of the initial pH as a function of the reaction temperature is shown on **Fig. 7**.

3.2. Experimental determinations

In parallel, blank experiments were carried out under argon or synthetic air (50 bar total pressure, 34 bar partial pressure of argon or air) at 200 °C in the absence of any catalyst. The results are presented on **Fig. 8**. The data point before zero time ($t = 0$) corresponds to the ammonia concentration in the solution just before heating the reaction mixture up to 200 °C, i.e. at ambient temperature

Table 6

Evolution of the equilibrium concentrations in $[H_3O^+]$, $[OH^-]$, $[NH_4^+]$, $[NH_3]$, and $[NH_3]_g$ and the pH as a function of temperature in the range 25–250 °C ($[NH_3]_0 = 60 \text{ mmol L}^{-1}$; $V_l = 150 \text{ mL}$, $V_g = 123 \text{ mL}$). For the calculations, the average values for K_b , K_w and K_H^{cc} were derived from **Tables 2–4**, respectively.

T (°C)	Concentrations (mmol L ⁻¹)					pH
	$[H_3O^+]$	$[OH^-]$	$[NH_4^+]$	$[NH_3]$	$[NH_3]_g$	
25	9.792×10^{-9}	1.021×10^0	1.021×10^0	5.895×10^1	4.204×10^{-2}	11.01
50	5.164×10^{-8}	1.053×10^0	1.053×10^0	5.886×10^1	1.056×10^{-1}	10.29
75	1.980×10^{-7}	1.007×10^0	1.007×10^0	5.880×10^1	2.309×10^{-1}	9.70
100	6.488×10^{-7}	9.159×10^{-1}	9.159×10^{-1}	5.871×10^1	4.525×10^{-1}	9.19
125	1.474×10^{-6}	7.984×10^{-1}	7.984×10^{-1}	5.854×10^1	8.099×10^{-1}	8.83
150	3.236×10^{-6}	6.727×10^{-1}	6.727×10^{-1}	5.823×10^1	1.345×10^0	8.49
175	6.841×10^{-6}	5.506×10^{-1}	5.506×10^{-1}	5.772×10^1	2.115×10^0	8.16
200	1.238×10^{-5}	4.394×10^{-1}	4.394×10^{-1}	5.703×10^1	3.089×10^0	7.91
225	2.102×10^{-5}	3.420×10^{-1}	3.420×10^{-1}	5.609×10^1	4.348×10^0	7.68
250	3.438×10^{-5}	2.592×10^{-1}	2.592×10^{-1}	5.493×10^1	5.874×10^0	7.46

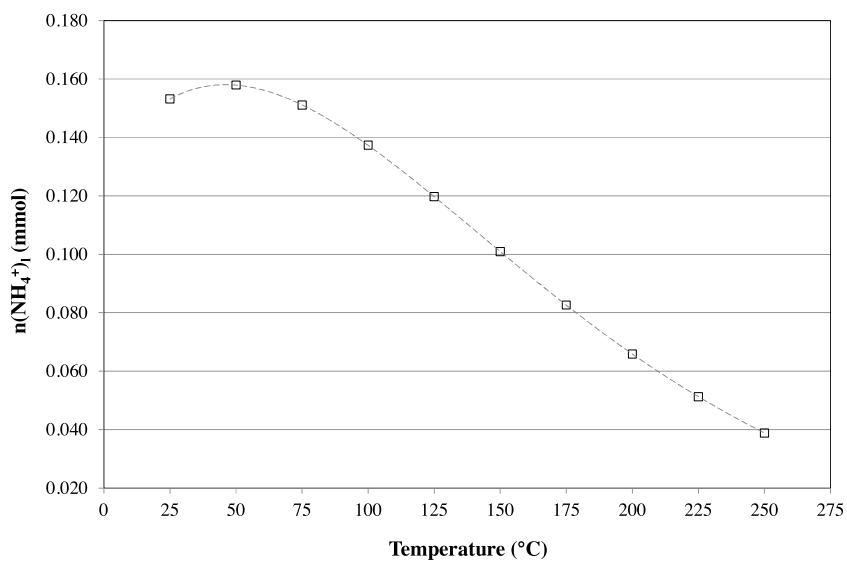


Fig. 4. Evolution of the number of mole of ammonium ion in the liquid phase ($n(\text{NH}_4^+)_l$) at the thermodynamic equilibrium as a function of temperature, in the range 25–250 °C ($[\text{NH}_3]_0 = 60 \text{ mmol L}^{-1}$; $V_l = 150 \text{ mL}$, $V_g = 123 \text{ mL}$).

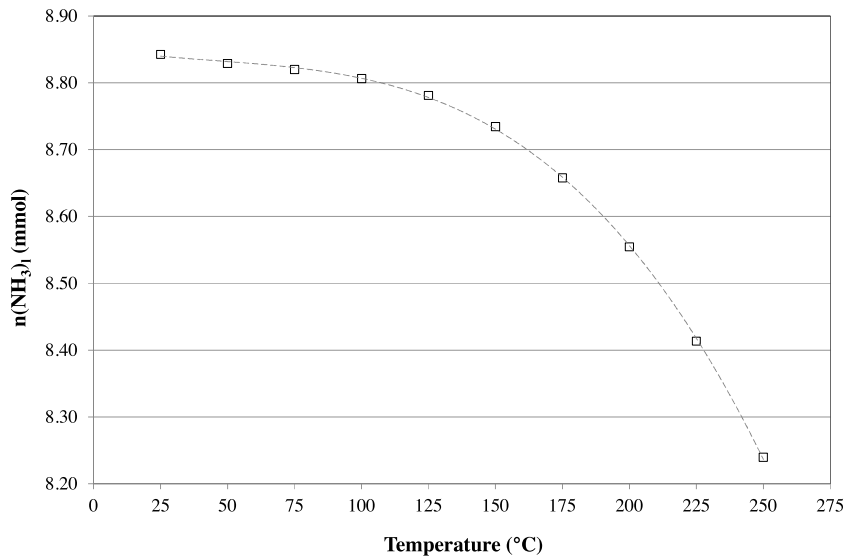


Fig. 5. Evolution of the number of mole of ammonia in the liquid phase ($n(\text{NH}_3)_l$) at the thermodynamic equilibrium as a function of temperature, in the range 25–250 °C ($[\text{NH}_3]_0 = 60 \text{ mmol L}^{-1}$; $V_l = 150 \text{ mL}$, $V_g = 123 \text{ mL}$).

Table 7

Evolution of the equilibrium composition in NH_4^+ in the liquid phase and NH_3 in the liquid and gas phases as a function of temperature in the range 25–250 °C, derived from Table 6 ($[\text{NH}_3]_0 = 60 \text{ mmol L}^{-1}$; $V_l = 150 \text{ mL}$, $V_g = 123 \text{ mL}$).

T(°C)	$n(\text{NH}_4^+)_l$ (mmol)	$n(\text{NH}_3)_l$ (mmol)	$n(\text{NH}_3)_g$ (mmol)
25	0.15	8.84	0.01
50	0.16	8.83	0.01
75	0.15	8.82	0.03
100	0.14	8.81	0.06
125	0.12	8.78	0.10
150	0.10	8.73	0.17
175	0.08	8.66	0.26
200	0.07	8.55	0.38
225	0.05	8.41	0.53
250	0.04	8.24	0.72

and atmospheric pressure. Upon heating the solution from room temperature to 200 °C, the total ammonia concentration in solution ($[\text{NH}_4^+] + [\text{NH}_3]_l$) measured via ion chromatography decreased

from 60 down to 50 mmol L⁻¹. This difference was attributed to the ammonia vaporization into the gas phase. Upon reaction under either argon or air at 200 °C, the ammonia concentration profiles were very similar and no significant ammonia oxidation was evidenced. After cooling down the reactor to ca. 25 °C, the ammonia concentration in solution returned to ca. 60 mmol L⁻¹. This later observation further indicated that ammonia did not get oxidized in the gas phase as well.

Additional tests were also performed in the presence of the bare TiO_2 and ZrO_2 supports (Fig. 9). Whatever the support, the same trends were observed as above. The ammonia concentration in the liquid phase at 200 °C stayed constant at ca. 50 mmol L⁻¹ and no oxidation took place.

3.3. Discussion

A reasonably good agreement was observed at 200 °C between the thermodynamic calculations and the experimental results,

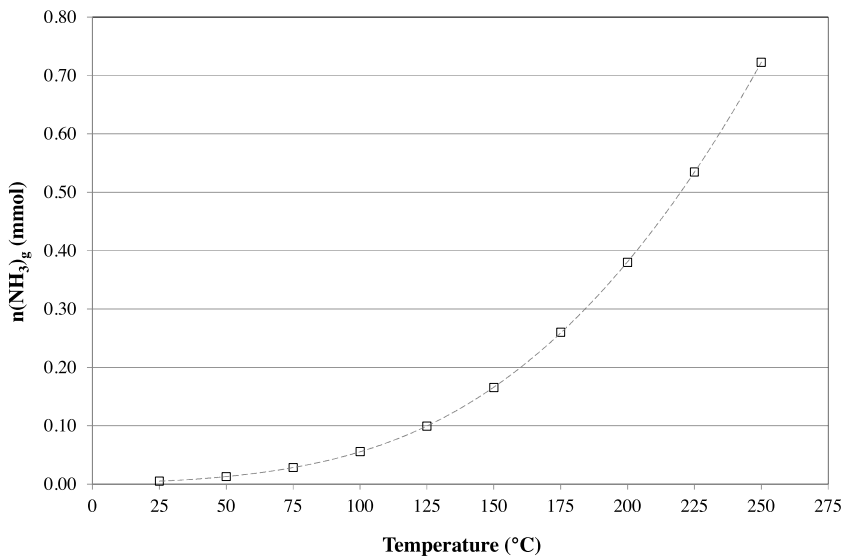


Fig. 6. Evolution of the number of mole of ammonia in the gas phase ($n(NH_3)_g$) at the thermodynamic equilibrium as a function of temperature, in the range 25–250 °C ($[NH_3]_0 = 60 \text{ mmol L}^{-1}$; $V_l = 150 \text{ mL}$, $V_g = 123 \text{ mL}$).

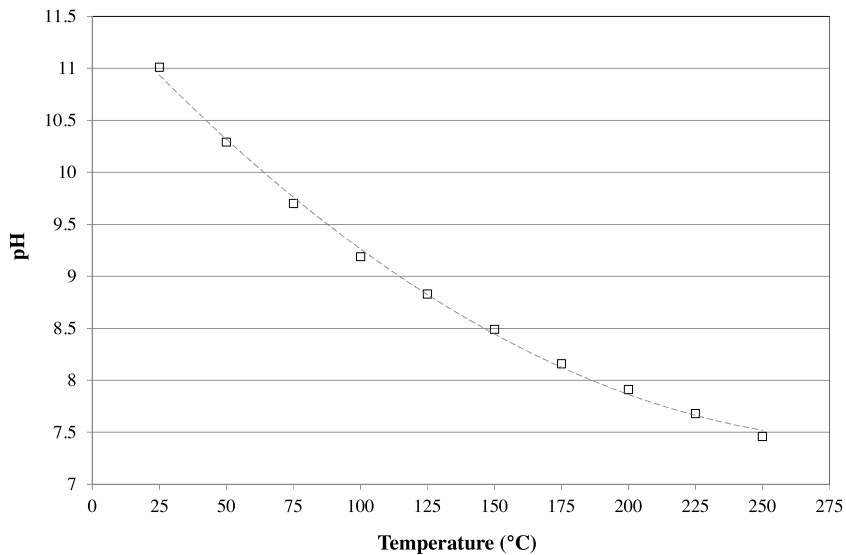


Fig. 7. Evolution of the pH of the reaction mixture as a function of temperature, in the range 25–250 °C.

especially considering the accuracy on the ion chromatography measurements. The largest discrepancy appeared for the ammonia concentration in the gas phase since the thermodynamic calculations predicted that the equilibrium concentration in ammonia in the gas phase ($[NH_3]_g$) is ca. 3.1 mmol L⁻¹ and the experimental concentration ($[NH_3]_{g,exp}$) was calculated to be ca. 12.2 mmol L⁻¹ from Eq. (13).

$$[NH_3]_{g,exp} = \frac{([NH_3]_{0,exp} \times V_l) - ([NH_3]_{l,exp} \times V_l)}{V_g} \quad (13)$$

This discrepancy was attributed to the major uncertainty on the Henry's constant, as already discussed in Section 3.1. Indeed, the calculation of $K_H(T)$ includes the constant $\frac{\Delta_{sol}H}{R}$ in the exponential term (Eq. (8)). This constant may vary between 1500 and 4400 K depending on the authors [22]. If $\frac{\Delta_{sol}H}{R}$ was considered to be equal to 4400 K for the thermodynamic calculations, the discrepancy between the calculated value for the ammonia concentration

in the gas phase and the experimental one would be reduced (5.8 vs. 12.2 mmol L⁻¹).

Finally, the thermodynamic calculations were much helpful to understand why the ammonia evaporation at 200 °C was quite limited compared to what could have been expected looking only at the pK_a of the ammonia molecule and the initial pH of the solution at ambient temperature under atmospheric pressure.

Moreover, looking at Table 7, we observed not only that ammonia was the most dominant species in the liquid phase in the whole temperature range, but also that the ammonia to ammonium ratio in the liquid phase sharply increased as the temperature increased from 25 up to 250 °C. This later information is of major importance since the most reactive species in catalysis is the ammonia form [11,13,23]. Indeed, this parameter could also partly contribute to the higher catalytic activity measured at higher temperature, in addition to the expected and predominant thermal effect (Arrhenius law).

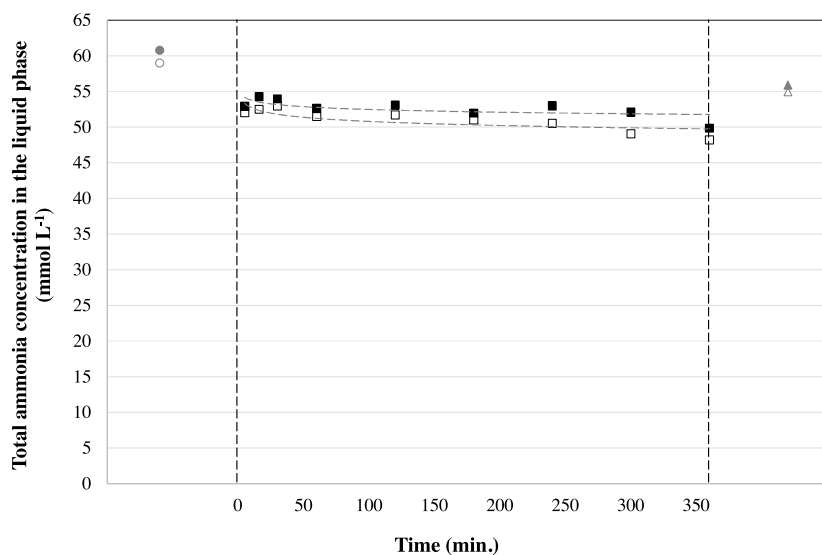


Fig. 8. Wet air oxidation of ammonia, in the absence of any catalyst, under argon (open symbols) or synthetic air (full symbols) at 200 °C ($[NH_3]_0 = 60 \text{ mmol L}^{-1}$; $V_l = 150 \text{ mL}$, $V_g = 123 \text{ mL}$, $pH_0 = 11$, total pressure = 50 bar, oxygen partial pressure under synthetic air = 6.8 bar).

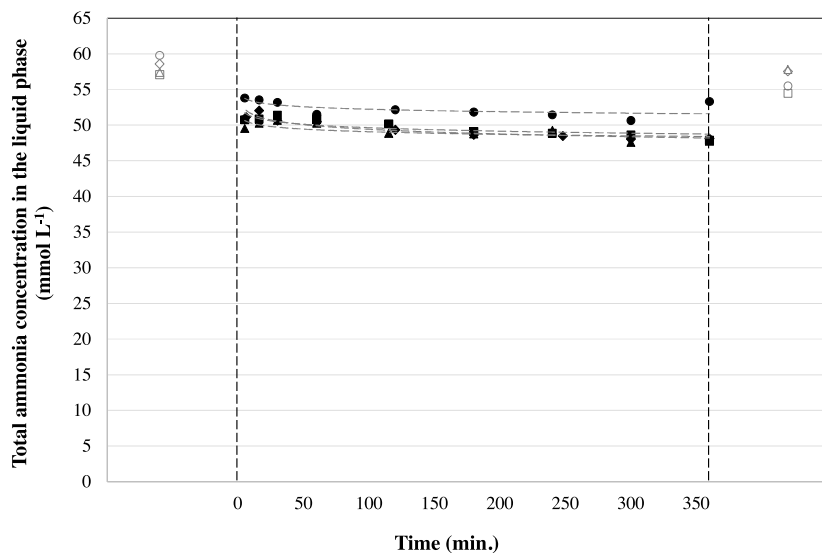


Fig. 9. Wet air oxidation of ammonia, over the bare metal oxide supports ($\blacktriangle TiO_2$, $\blacksquare ZrO_2$, $\blacklozenge CeO_2$, $\bullet Ce_{0.7}Zr_{0.3}O_2$), under synthetic air at 200 °C ($[NH_3]_0 = 60 \text{ mmol L}^{-1}$; $V_l = 150 \text{ mL}$, $V_g = 123 \text{ mL}$, $pH_0 = 11$, total pressure = 50 bar, oxygen partial pressure under synthetic air = 6.8 bar).

4. Conclusions

Taking into account the whole reaction system, the mass and charge balances, the acid-base constant of ammonia, the self-ionization constant of water and the gas-phase equilibrium constant for ammonia, the equilibrium concentrations in ammonia and ammonium ion in the liquid and gas phases could be calculated in the temperature range 25–250 °C. A valuable procedure was developed and described in this manuscript. The same approach could be easily applied for a better description of any liquid phase reaction where liquid-liquid, gas-liquid and acid-base equilibria are involved.

Although basic thermodynamic data were pretty scarce and a large variation was reported for the Henry's constant, a reasonably agreement was obtained with the results acquired upon blank experiments and in the presence of inert catalyst supports. Considering our experimental setup and the applied reaction conditions, it appeared that ammonia evaporation was limited to ca. 2.9 mol%,

indicating that any reaction would mainly occurred in the liquid phase. Moreover, in the liquid phase, ammonia (96.2 mol%) strongly dominated over ammonium ions (0.9 mol%). This latter point could partly explain the high activity observed in the catalytic wet air oxidation reaction since the molecular form of ammonia was shown to be the most reactive.

Finally, such preliminary thermodynamic calculations were extremely useful to understand better the evolution of the different equilibria as a function of temperature and their impact on the reaction medium composition. Getting a deeper insight into these equilibria was also crucial since it may directly and strongly impact on the catalysis.

Acknowledgements

The authors gratefully acknowledge the French Ministry for Higher Education and Research for the Ph.D. grants awarded to Cédric Lousteau for the period 2010–2013 and Hana Ayadi for the

period 2014–2017. Dr. Alain Perrard's help was also very much precious while dealing with the thermodynamic calculations.

References

- [1] Mineral Commodity Summaries, U.S. Department of Interior, U.S. Geological Survey, 2016 <http://minerals.usgs.gov/minerals/pubs/mcs/2016/mcs2016.pdf>.
- [2] S. Obaid-Ur-Rehman, S.A. Beg, *J. Environ. Sci. Health: Part A* 25 (1990) 343–365.
- [3] A. Hedström, *J. Environ. Eng.* 127 (2001) 673–681.
- [4] M. Rozic, S. Cerjan-Stefanovic, S. Kurajica, V. Vancina, E. Hodzic, *Water Res.* 34 (2000) 3675–3681.
- [5] W. Verstraete, S. Philips, *Environ. Pollut.* 102 (1998) 717–726.
- [6] U. van Dongen, M.S.M. Jetten, M.C.M. Loosdrecht, *Water Sci. Technol.* 44 (2001) 153–160.
- [7] J. Hoigne, H. Bader, *Environ. Sci. Technol.* 12 (1978) 79–84.
- [8] P.C. Singer, W.B. Zilli, *Water Res.* 9 (1975) 127–134.
- [9] L. Huang, L. Li, W. Dong, Y. Liu, H. Hou, *Environ. Sci. Technol.* 42 (2008) 8070–8075.
- [10] M. Altomare, E. Selli, *Catal. Today* 209 (2013) 127–133.
- [11] J. Qin, K. Aika, *Appl. Catal. B: Environ.* 16 (1998) 261–268.
- [12] J. Taguchi, T. Okuhara, *Appl. Cata. A: Gen.* 194 (2000) 89–97.
- [13] S. Cao, G. Chen, X. Hu, P.L. Yue, *Catal. Today* 88 (2003) 37–47.
- [14] J. Barbier Jr., L. Oliviero, B. Renard, D. Duprez, *Catal. Today* 75 (2002) 29–34.
- [15] R. Ukkonen, B.F.M. Kuster, J.C. Schouten, R.A. van Santen, *Appl. Catal. B: Environ.* 23 (1999) 45–57.
- [16] R.G. Bates, G.D. Pinching, *J. Am. Chem. Soc.* 72 (3) (1950) 1393–1396.
- [17] J.R. Fisher, H.L. Barnes, *J. Phys. Chem.* 76 (1) (1972) 90–99.
- [18] H.S. Harned, W.J. Hamer, *J. Am. Chem. Soc.* 55 (6) (1933) 2194–2206.
- [19] J.V. Dobson, H.R. Thirsk, *Electrochim. Acta* 16 (1971) 315–338.
- [20] C. Tsionopoulos, D.M. Coulson, L.B. Inman, *J. Chem. Eng. Data* 21 (2) (1976) 190–193.
- [21] M.E. Jones, *J. Phys. Chem.* 67 (5) (1963) 1113–1115.
- [22] R. Sander, *Compilation of Henry's Law Constants for Inorganic and Organic Species of Potential Importance in Environmental Chemistry*, Air Chemistry Department, Max-Planck Institute of Chemistry, 1999 <http://www.henrys-law.org/henry-3.0.pdf>.
- [23] D.K. Lee, J.S. Cho, W.L. Yoon, *Chemosphere* 61 (4) (2005) 573–578.